Engineering with Computers (2022) 38 (Suppl 2):S1331–S1347
https://doi.org/10.1007/s00366-020-01277-4

ORIGINAL ARTICLE

Quick integrative optimizers for minimizing the error of neural computing in pan evaporation modeling

Hossein Moayedi[1,2] · **Soheil Ghareh**[3] · **Loke Kok Foong**[4,5]

Received: 14 October 2020 / Accepted: 29 December 2020 / Published online: 23 January 2021

Abstract
To achieve an efficient methodology for approximating pan evaporation (E_P), this study offers two metaheuristic-integrated predictors. Shuffled complex evolution (SCE) and electromagnetic field optimization (EFO) are two of the fastest metaheuristic algorithms that are synthesized with artificial neural network (ANN). By doing this, the ANN is optimized in a noticeably shorter time compared to its integration with other metaheuristic techniques. Five-year climatic data of the Bakersfield station (California, USA) with an 80:20 ratio are used for developing and testing the methods. The proposed hybrids are implemented with appropriate population sizes (20 and 35 for the SCE and EFO, respectively) and their results are compared to a single ANN. Accuracy evaluation (correlation coefficients > 0.99) professed that the neural network with both conventional and sophisticated trainers is a competent approach for the E_P simulation. Besides, it was observed that the error of prediction by the ANN-SCE and ANN-EFO is 6.02 and 9.27% lower than the single ANN, respectively. Therefore, the used strategies can enhance the applicability of the ANN. The time elapsed in the optimization using SCE and EFO was 479.0 and 281.9 s, respectively. A comparison between these algorithms revealed that the EFO is both a faster and more accurate optimizer. The ANN-EFO is accordingly recommended as a new efficient model for predicting the E_P.

Keywords Water management · Evaporation · Neural modeling · Metaheuristic optimization

1 Introduction

Evaporation is known as one type of vaporization that happens on the surface of a liquid as it converts into the gas phase [1–4]. As a significant environmental and climatic concern, and to minimize the negative its effects on the environment, the water-loss step of the water cycle, are extensively discussed [5–14]. There have been many case studies working on current worldwide environmental concerns [15–19]. In this sense, and during recent decades, artificial intelligence has proved to be one of the most popular methods for the indirect analysis of environmental engineering-based factors [20–27], and more specifically the pan evaporation (E_P) [28, 29]. Fuzzy-based tools [30–32], regression-based methods [33, 34], neural learning [35–37], and support vector approaches [38–40] are well-known techniques that have been highly regarded by experts. Further applications of intelligent tools can be found in different fields such as in engineering [41–46], structural health monitoring [47–52], reinforced concrete structure performance [53–56], computer vision techniques such as machine vision [57], moving object detection [58, 59], image enhancement [60, 61], air quality [62, 63], energy [64–71], computational image processing [72–78], groundwater remediation strategies [79], big-data in traffic management [80], prefabricated walls [71–83], socially aware networks [84], climatic change [85, 86], or even in medical sciences [77–95]. Recently, programmers have used various metaheuristic algorithms for

✉ Loke Kok Foong
lokekokfoong@tdtu.edu.vn

Hossein Moayedi
hosseinmoayedi@duytan.edu.vn

1 Institute of Research and Development, Duy Tan University, Da Nang 550000, Vietnam

2 Faculty of Civil Engineering, Duy Tan University, Da Nang 550000, Vietnam

3 Department of Civil Engineering, Payam Noor University, Tehran, Iran

4 Department for Management of Science and Technology Development, Ton Duc Thang University, Ho Chi Minh City, Vietnam

5 Faculty of Civil Engineering, Ton Duc Thang University, Ho Chi Minh City, Vietnam

optimization aims [96, 97]. A particular application of these techniques is hybridizing the existing predictive models. In this sense, hybrid kernel extreme learning machine [98], fruit fly optimization [99], bacterial foraging optimization [100], many-objective sizing optimization [101–104], Harris hawks optimizer [105], data-driven robust optimization [106], multi-objective 3-d topology optimization [107], global numerical optimization [108], moth-flame optimization [109] are some good examples of machine learning, conventional neural network, and hybridized optimization algorithms. Different studies are trying to extend the superiority of prediction techniques such as deep learning [110–114], feature selection [115, 116], or feature extraction [117–119]. Arunkumar et al. [120] employed three data mining approaches including artificial neural network (ANN), model tree (MT), and genetic programming (GP) for developing E_P evaluative tools. With a correlation of 0.959, the GP was stronger than other methods. This is while the ANN was found to be more suitable for cause–effect mapping. Alsumaiei [121] applied an ANN to the prediction of the daily rate of E_P in hyper-arid climates in Kuwait. With reference to the obtained Nash–Sutcliffe coefficients (varying in [0.405, 0.755]), the ANN could satisfactorily handle this task. The applicability of multivariate adaptive regression spline (MARS) and MT incorporated with maximum overlap discrete wavelet transform was examined by Ghaemi et al. [122]. As a result of this hybridization, significant decreases were observed in the error of both standard MARS and MT. Likewise, a combination of response surface method (RSM) and support vector regression (SVR) was proposed by Keshtegar et al. [123] for E_P modeling. According to the accuracy measures, this model outperformed single methods and a capable ANN, namely multilayer perceptron (MLP).

By combining the nature-inspired searching algorithms, optimal configurations of the intended models are achieved. This measure also prevents computational threats like local minima [124]. Roy et al. [125], for example, used biogeography-based optimization (BBO), teaching–learning-based optimization (TLBO), firefly algorithm (FFA), and particle swarm optimization (PSO) for optimizing an adaptive neuro-fuzzy inference system (ANFIS) applied to evapotranspiration prediction. Gocić et al. [126] achieved two powerful methodologies for reference evapotranspiration modeling by combining the support vector machine (SVM) with FFA and wavelet technique. They compared the performance of these two hybrids with ANN and GP, and witnessed the better performance of the FFA-SVM and SVM-wavelet. Mohammadi and Mehdizadeh [127] created a hybrid of whale optimization algorithm (WOA) and SVR for the same purpose in Iran. They also showed that random forest (RF) is a good tool for input evaluation. With normalized root-mean-square errors (RMSEs) of 5.466, 9.958, and 5.412% calculated for Isfahan, Urmia, and Yazd stations, respectively, the proposed method outperformed seven other predictors including typical SVR. In a different study, Liu et al. [128] proposed a searching algorithm to solve box constrained global optimization problems. They used an example of structural design.

As for the ANNs, many scholars have coupled these tools with nature-inspired optimizers for hydrological simulations [129–131]. A hybrid of FFA-ANN was proposed by Ashrafzadeh et al. [132] for the E_P approximation. Due to the better performance of the ensemble model relative to the conventional ANN, they concluded that retrofitting this processor with the FFA is a promising way toward accuracy enhancement. Tikhamarine et al. [133] predicted reference evapotranspiration in India and Algeria using five ensembles of ANN with PSO, WOA, grey wolf optimizer (GWO), ant lion optimizer (ALO), and multi-verse optimizer (MVO). A comparative assessment of the results pointed out the superiority of the GWO for training the ANN. A similar application of the GWO and WOA, as well as genetic algorithm (GA), was presented by Seifi and Soroush [134]. They coupled these optimizers with ANN for predicting the E_P in different parts of Iran. Among the metaheuristic-based ANNs, those trained the GA outperformed the WOA and GWO.

Despite the adequate competency shown by metaheuristic approaches in optimizing standard predictors, they mostly take a large time for this process. Due to the importance of time-efficiency in engineering assessments, this study offers optimal hybrids for the E_P prediction. To this end, the optimization of an ANN is assigned to two fast metaheuristic algorithms, namely shuffled complex evolution (SCE) and electromagnetic field optimization (EFO). While these algorithms have been effectively employed for optimization objectives [135], no prior effort can be found regarding their application in the E_P estimation.

2 Data acquisition and statistics

As is known, data provision is a crucial step in machine learning implementation for predicting any parameter [136]. Therefore, the data should be obtained from a valid source. Generally, besides the intended parameter(s) (i.e., to be predicted), some factors are required for creating a database. These factors are selected based on a logical (here dependent-independent) relationship and play the role of influencing factors for the intended parameter in the real world. In the case of this study, the E_P is the dependent parameter influenced by wind speed (S_W), air temperature (T_A), daylight pressure (P_D), solar radiation (R_S), and daylight humidity (H_D). These independent factors are called inputs hereafter.

The climatic records belonging to a 5-year period are used in this work. More clearly, the values of E_P, S_W, T_A, P_D, R_S, and H_D from January 01, 1986 to December 31, 1990

were downloaded from the website of the US environmental protection agency (http://www.epa.gov). Figure 1 shows the variation of the target parameter (i.e., the E_P) in this period. As is seen, this figure is divided into two separate parts by the name training and testing. The training data cover the first 4 years and the fifth year is dedicated to testing data. The reason for doing this is to evaluate the generalizability of the models using new climatic conditions. In this regard, once the models capture the E_P pattern by analyzing the training data (1986–1989), they are asked to predict the E_P for the year 1990. Table 1 gives the statistical description of both datasets.

Finally, in this section, Fig. 2 shows the location of the studied station. It is the Bakersfield station located in the central part of Kern County, California, with a warm and semi-arid climate [137]. The longitude and latitude are 119° 03′ W and 35° 25′ N, respectively. Also, the elevation in this area is around 151 m above sea level. According to Table 1, the average temperature was around 18.3 °C over the selected time. Also, the E_P ranged in [0.3, 20.5] mm with an average of 7.8 and 7.9 mm in the training and testing period, respectively.

3 Methodology

3.1 The SCE

The SCE was developed by Duan et al. [138] as an efficient and simple metaheuristic optimizer. This algorithm relies

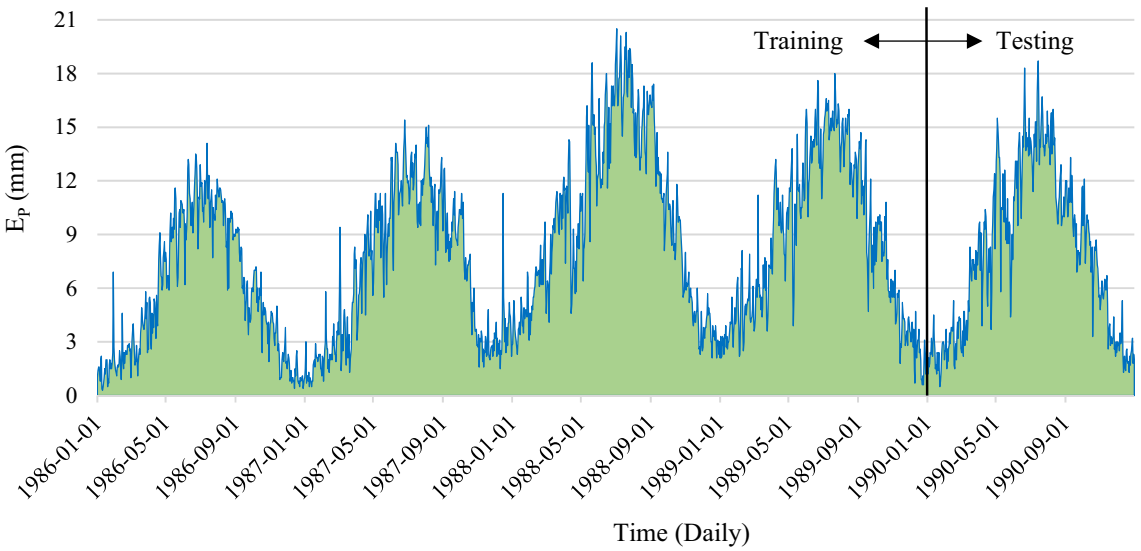

Fig. 1 The E_P variation in the intended period

Table 1 Statistical indices of data in both periods

Group	Factor	Unit	Indicator				
			Mean	Standard deviation	Skewness	Minimum	Maximum
Training	S_W	mi/h	10.3	3.8	0.1	3.9	27.5
	T_A	°C	18.3	7.8	− 0.1	0.4	34.3
	P_D	Kpa	99.8	0.5	0.4	97.7	101.6
	R_S	Langley	445.4	196.7	− 0.1	64.8	760.2
	H_D	%	48.2	18.1	0.7	15.0	100.0
	E_P	mm	7.8	4.6	0.3	0.3	20.5
Testing	S_W	mi/h	13.8	1.5	0.5	8.7	19.5
	T_A	°C	18.1	8.4	− 0.1	− 2.8	35.3
	P_D	Kpa	99.8	0.5	0.7	98.8	101.2
	R_S	Langley	458.9	187.5	− 0.1	104.9	753.3
	H_D	%	47.6	16.4	0.5	20.0	99.0
	E_P	mm	7.9	4.5	0.2	0.5	18.7

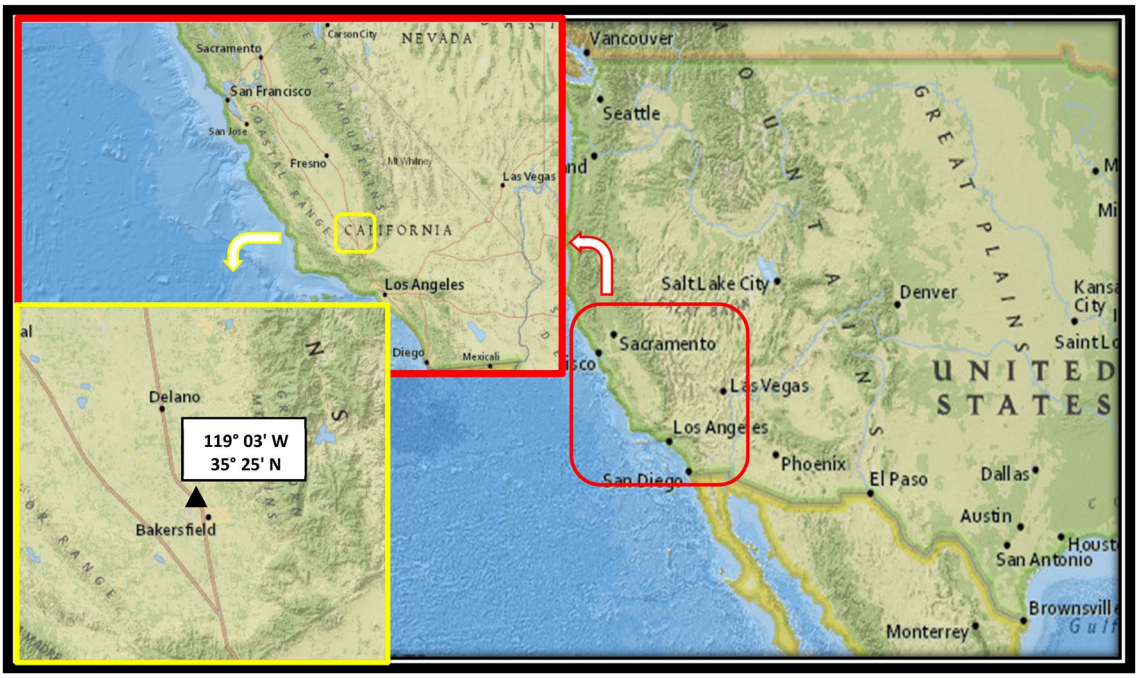

Fig. 2 Location of the Bakersfield station (WBAN Number: 23155)

on the synthesizing four concepts, including (a) combining probabilistic and deterministic techniques, (b) evolving a set of points (called complex) that span the space toward an optimal situation, (c) performing a competitive evolution strategy, and (d) shuffling the complex [139]. Like other algorithms, each member represents a possible solution to the given problem. For doing the optimization, first, initial individuals are equally divided into a number of complexes. A local optimum solution is discovered by each complex by executing downhill simplex method. After repeating this process for new points, these solutions are then processed and collected to attain a global response.

In the first step, the problem and parameters are initialized. Given $OF(H)$ as the objective function, Eq. 1 expresses how the problem is defined.

$$\text{Min OF}(H) = \sum_{x} \frac{\left|H_i + h_{px} - h_{Lx} - H_j\right|^{\left(\frac{1}{n}\right)+1}}{R_x^{\frac{1}{n}}} + \left(\frac{1}{n}+1\right)\sum_{j} q_{oj}(H_j), \tag{1}$$

where H symbolizes the group of each decision parameter. In the second step, the initial population is generated as follows:

$$H(i,j) = H_{\min}(i,j) + \text{rand}\left(H_{\min}(i,j) - H_{\max}(i,j)\right), \tag{2}$$

in which rand is a random number uniformly distributed from 0 to 1, and $H_{\min}(i,j)$ and $H_{\max}(i,j)$ denote the lower and upper bounds of j at the ith node. In the following, the OF(H) is calculated for all individuals. Given N as the number of unknown nodes, the population matrix can be expressed as follows:

$$P = \begin{bmatrix} C_1 \\ C_2 \\ \vdots \\ C_{\text{NP}} \end{bmatrix} = \begin{bmatrix} H_1^1 & H_2^1 & \cdots & H_N^1 \\ H_1^2 & H_2^2 & \cdots & H_N^2 \\ \vdots & \vdots & \ddots & \vdots \\ H_1^{\text{NP}} & H_2^{\text{NP}} & \cdots & H_N^{\text{NP}} \end{bmatrix}. \tag{3}$$

In the third step, the algorithm sorts S solutions with respect to the objective functions. Next in the fourth step, it partitions these solutions into M complexes, so that each of these units contains m points. In this regard, the points by the number $M(k-1)+1$ go to the first complex, the points by the number $M(k-1)+2$ go to the first complex, and so on ($k=1, 2, \ldots, m$). After implementing the competitive complex evolution as the fifth step, the sixth step is dedicated to shuffling the complexes. Finally, termination criteria are checked to stop repeating steps 3, 4, and 5 [140]. The SCE is also explained in earlier studies [141, 142].

3.1.1 The EFO

The EFO draws on electromagnetics rules to provide a fast and capable optimizer. Abedinpourshotorban et al. [143] developed the EFO in 2016. In a cooperative process, the population, which is composed of electromagnet particles (EMPs), enhances the positions to replace poor solutions

with promising ones. The interaction between the EMPs is based on the attraction–repulsion rule.

The optimization strategy in the EFO can be expressed in four major stages. First, a certain number of EPMs are randomly generated. Concerning their fitness, the EMPs are organized. The next stage is dedicated to the classification of individuals. Three groups of EMPs are formed, so that the first group, called positive field, contains the best-fitted individuals; the second group, called negative field, contains the worst individuals; and the third group, called neutral field, contains the individuals with low negative polarities. Producing and organizing new EMPs are crucial steps of the EFO. The production process is illustrated in Fig. 3.

The bounds of the new member have to comply with the existing space. In other words, once it is not limited to space, another EMP is produced. Given n as the number of EMPs and GR as the golden ratio, the production process can be mathematically expressed as follows:

$$\mathrm{EMP}_n^{\mathrm{new}} = \mathrm{EMP}_n^{K_n} + \left((\mathrm{GR} * \mathrm{rand}) * D_n^{P_n K_n}\right) - \left(\mathrm{rand} * \left(D_n^{N_n K_n}\right)\right), \tag{4}$$

where rand is a random value ranging in [1]. Also, $D_n^{N_n K_n}$ and $D_n^{P_n K_n}$ are obtained by the following equations:

$$D_n^{N_n K_n} = \mathrm{EMP}_n^{N_n} - \mathrm{EMP}_n^{K_n}, \tag{5}$$

$$D_n^{P_n K_n} = \mathrm{EMP}_n^{P_n} - \mathrm{EMP}_n^{K_n}, \tag{6}$$

where $\mathrm{EMP}_n^{N_n}$, $\mathrm{EMP}_n^{P_n}$, and $\mathrm{EMP}_n^{K_n}$ stand for the negative, positive, and neutral electromagnet, respectively.

In the last step, a random number is generated and compared to the parameter R_{Rate} to decide about the replacement process. Note that R_{Rate} is the probability of changing an electromagnet (of the produced EMP) with a random one. If R_{Rate} is larger than the random value, the replacement occurs [144]. Further explanations about the EFO mechanism can be found in Refs. [145, 146].

3.2 Hybridization

The SCE and EFO aim to train the ANN for predicting the E_{P}. For this purpose, a valid ANN structure should be determined as the skeleton of the hybrid models. The ANN structure suggested for this work is shown in Fig. 4. It is an MLP network with five inputs and one output. As is seen, there are five neurons in the middle layer that are determined after a trial and error proceeding. The suitability of this structure has also been professed in earlier studies [147]. In such networks, the calculation is carried out by the neurons by applying an activation function to a linear combination of weights, biases, and input values. The same process is executed by the subsequent neurons to produce the overall response (i.e., E_{P}) [148–150]. According to Table 2, 36 parameters are involved in the prediction procedure. Therefore, each of the SCE and EFO should tune 36 parameters to attain an optimal ANN.

In metaheuristic algorithms, an iterative strategy is taken for improving the quality of the results. The goodness of the response in each iteration (i.e., the weights and biases) is evaluated by measuring the accuracy of training. Note that training data are used for this process. The algorithm tries to increase the accuracy by achieving a more promising solution to the ANN problem, and eventually, it is terminated somewhere. The last response of the algorithm builds the optimal ANN. The trained hybrids, called ANN-SCE and ANN-EFO, then predict the E_{P} for the testing period.

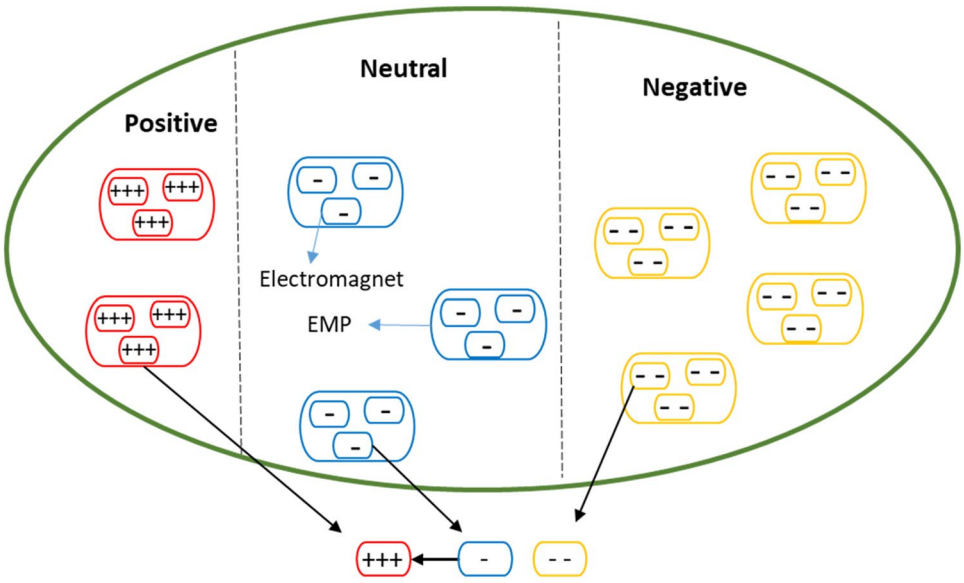

Fig. 3 Generating new members in the EFO

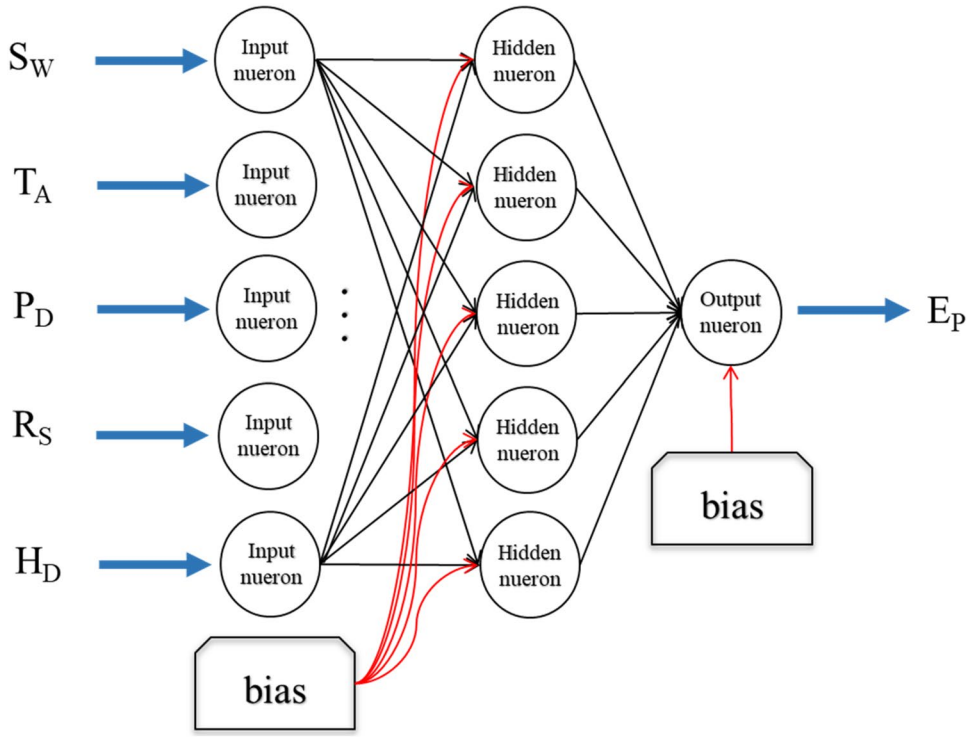

Fig. 4 The suggested ANN for hybridization

Table 2 The number of parameters in the suggested ANN

Parameter	Weight		Bias	
Location	Input-hidden	Hidden-output	Hidden	Output
Number	5×5=25	5×1=5	5	1
Sum	30		6	

3.3 Accuracy assessment indices

To have a valid assessment of the prediction results, different accuracy criteria can be defined. In this work, the error of prediction is measured by two standard criteria, namely root-mean-square error (RMSE) and mean absolute error (MAE). A percentage form of the MAE, called mean absolute percentage error (MAPE), is also used to give the relative error. Given Error as the difference between the recorded E_P ($E_{P_{\text{Record}}}$) and modeled E_P ($E_{P_{\text{Model}}}$), these criteria are expressed by the following equations:

$$\text{MAE} = \frac{1}{Z}\sum_{i=1}^{Z}|\text{Error}_i| \tag{7}$$

$$\text{RMSE} = \sqrt{\frac{1}{Z}\sum_{i=1}^{Z}[\text{Error}_i]^2} \tag{8}$$

$$\text{MAPE} = \frac{1}{Z}\sum_{i=1}^{Z}\left|\frac{\text{Error}_i}{E_{\text{P}_{\text{Record}_i}}}\right| \times 100, \tag{9}$$

where Z stands for the number of days.

Moreover, Eq. 10 expresses Pearson correlation coefficient (PCC) that is used for assessing the agreement between the $E_{P_{Record}}$ and $E_{P_{\text{Model}}}$:

$$\text{PCC} = \frac{\sum_{i=1}^{Z}\left(E_{\text{P}_{\text{model}_i}} - \overline{E_{\text{P}_{\text{model}}}}\right)\left(E_{\text{P}_{\text{Record}_i}} - \overline{E_{\text{P}_{\text{Record}}}}\right)}{\sqrt{\sum_{i=1}^{Z}\left(E_{\text{P}_{\text{model}_i}} - \overline{E_{\text{P}_{\text{model}}}}\right)^2}\sqrt{\sum_{i=1}^{Z}\left(E_{\text{P}_{\text{Record}_i}} - \overline{E_{\text{P}_{\text{Record}}}}\right)^2}}. \tag{10}$$

4 Results and discussion

4.1 Training results

The optimization mechanism was explained in Sect. 3.2. Based on the behavior of the used algorithms, different measures are taken for the implementation. As shown in Fig. 5a shows, for the ANN-SCE, eight values, including 2, 5, 10, 15, 20, 50, 100, and 200, are considered as the population size (N_P). It is observed that all tested networks reach a relatively stable convergence after 600 iterations. The magnified section illustrates that the response of $N_P=20$ achieved the lowest objective function (i.e., the RMSE in this case). Therefore, this network represents the proposed

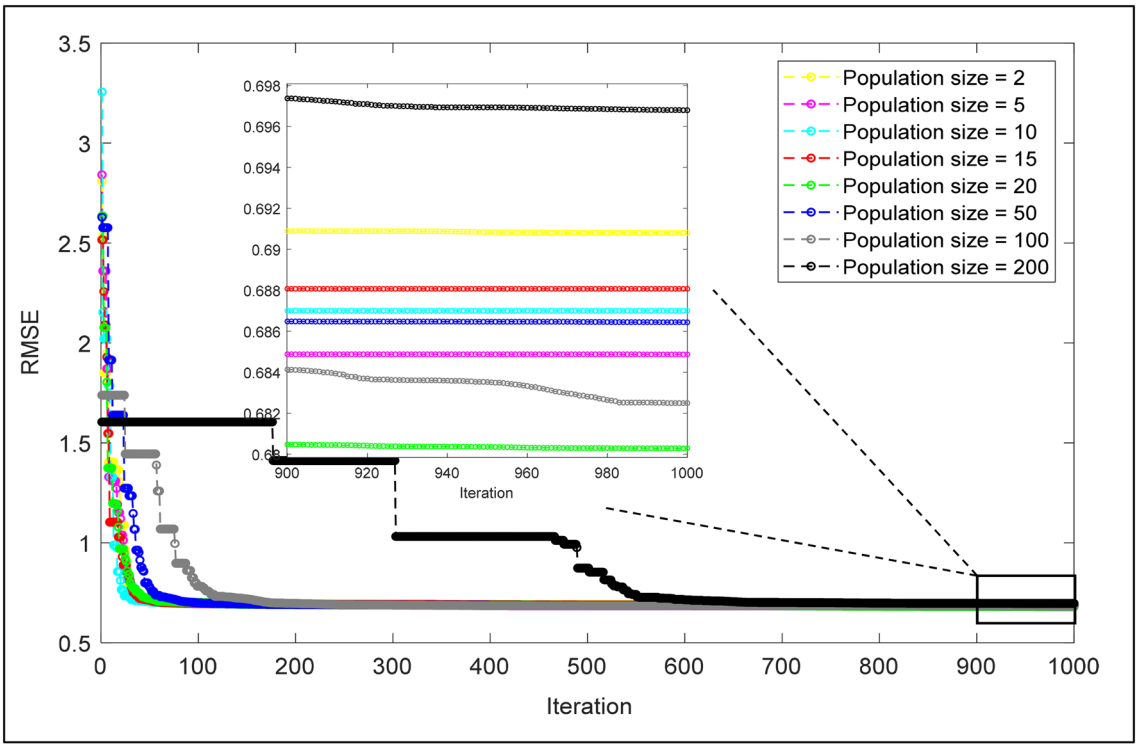

(a)

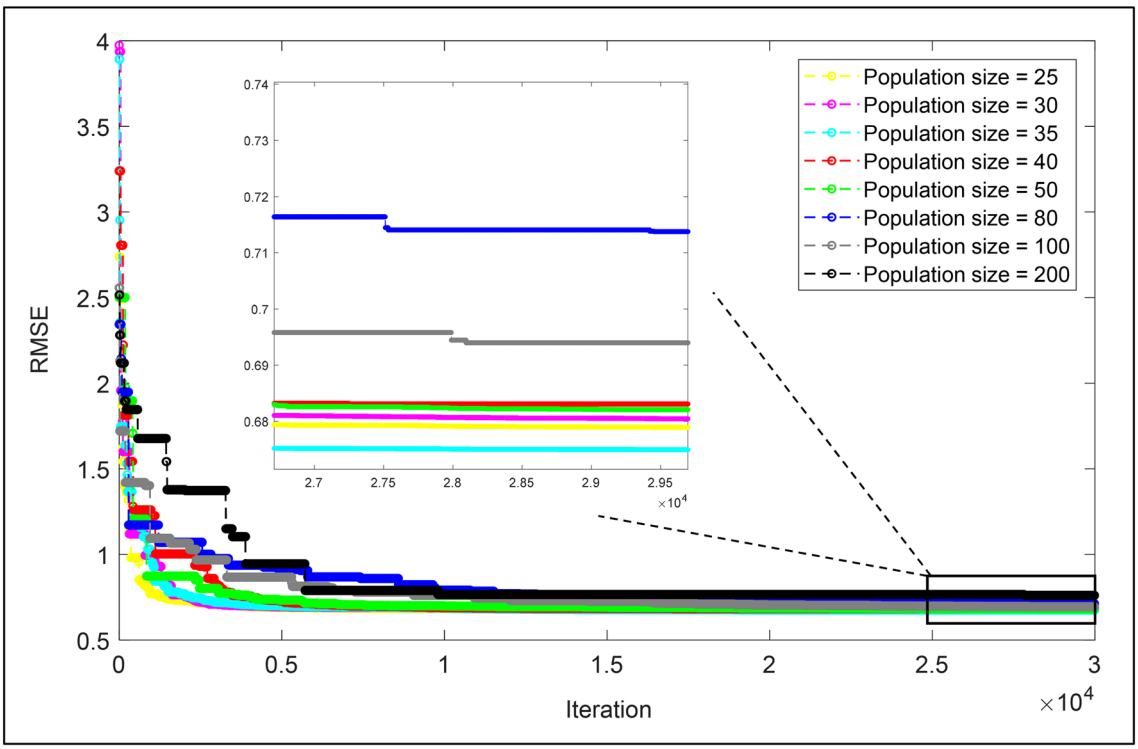

(b)

Fig. 5 Optimization of ANN using different N_ps of the **a** SCE and **b** EFO

ANN-SCE. As for the ANN-EFO, Fig. 5b shows the convergence curves for the N_Ps of 25, 30, 35, 40, 50, 80, 100, and 200. Due to the same reason, the network with $N_P = 35$ is selected to represent the ANN-EFO. A distinction between the implementation of these two algorithms is the number of iterations, which, based on their behaviors, is selected to be 1000 and 30,000 for the SCE and EFO, respectively. A single ANN trained by the Levenberg–Marquardt [151] is also considered as a benchmark to validate the performance of the used metaheuristic algorithms.

Figure 6 shows the training results in terms of error values (the same as Error explained above). In this phase, the RMSEs calculated for the single ANN, ANN-SCE, and ANN-EFO were 0.6958, 0.6802, and 0.6749, respectively. Likewise, the MEAs were 0.6080, 0.5954, and 0.5901. It indicates excellent training provided by all three strategies (i.e., LM, SCE, and EFO).

The high quality of training can also be confirmed by the PCCs of 0.98888, 0.98917, and 0.98934. However, by comparison, it can be derived that the SCE and EFO have made stronger ANNs. It implies that the ANN can be properly improved by metaheuristic techniques. It is due to the more suitable responses found by the SCE and EFO. These responses, as explained, comprise the neural parameters that reveal the intricate relationship between the E_P and S_W, T_A, P_D, R_S, and H_D (Fig. 4).

4.1.1 Testing results

The testing inputs were then given to the built networks to estimate the E_P for the year 1990. Regarding the fact that the networks had not come across these data, their performance in this section represents the generalizability of their knowledge. The results are assessed in the same way as the training phase. Figure 7 depicts the obtained errors. Having a look at the actual range of testing E_Ps in Table 1 (i.e., [0.5, 18.7] mm) and comparing it with the calculated errors demonstrate that all three models can elegantly estimate the E_P pattern in the testing period. In this regard, the RMSEs were 1.5647, 1.4764, and 1.4239. A low range of MAEs, i.e., 1.4947, 1.4047, and 1.3561, is another indicator of the high accuracy for all applied models. Moreover, the histogram charts show a suitable frequency of error values.

Furthermore, the agreement between the E_Ps recorded in the testing period and those estimated by the used models is graphically shown in Fig. 8. As is seen, the products are strongly correlated with real-world data. Referring to the obtained PCCs of 0.99838, 0.99824, and 0.99802, all three models enjoy a very good potential for prediction.

Moreover, Table 3 gives a correlation-based assessment of the testing results from a seasonal point of view. Based on the calculated coefficients of determination (R^2s), the models have done a very good prediction for all seasons.

Comparing the testing results of the ANN with hybrid models (i.e., ANN-SCE and ANN-EFO) reveals that although the obtained PCCs have slight differences, both error criteria indicate a significantly more accurate prediction for the ANNs trained by the SCE and EFO. It is even more highlighted when the single ANN is evaluated versus the EFO-ANN. In detail, letting the ANN be trained by the SCE and EFO resulted in around 5.64 and 9.00% reduction of RMSE and nearly 6.02 and 9.27% reduction of MAE, respectively. It reflects the higher capability of metaheuristic-trained ANNs in predicting the daily E_P. This finding becomes even more noticeable after knowing that the SCE and EFO are two of the fastest optimizers. The matter of time-effectiveness is discussed in the next section.

4.2 Comparison

The objective of the study was met after the above assessments. The ANN, which is a popular predictive model for the E_P modeling, experienced appreciable improvements in the accuracy of prediction by incorporating with the SCE and EFO metaheuristic techniques. Depending on different parameters like the type of problem, the number of variables, and the size of data, these algorithms mostly take a considerable time for attaining optimal solutions [152]. Some long calculations regarding ANN optimization can be mentioned for teaching–learning-based optimization and cuckoo optimization algorithm [65], spotted hyena optimizer [153], wind-driven optimization [154], etc. In contrast, scholars like Zheng et al. [155] have reached their desired optimization using the SCE in a shorter time.

In this work, the time taken by the SCE and EFO was about 479.0 and 281.9 s, respectively (on an Intel core i7 64-bit operating system with 16 gigs of RAM). It means that the EFO is a faster algorithm than SCE. Moreover, based on the lower values of the RMSE and MAE obtained for the ANN-EFO, the EFO can also be pointed out as a more capable algorithm, too.

4.3 Importance assessment

To investigate the effect of each input factor, a bagged ensemble of 200 regression trees is executed. The results are shown in Fig. 9. As is seen, S_W plays the most important role in the E_P simulation, while the lowest effect is exerted by the P_D factor. Also, the effect of three other factors can be considered as relatively gentle.

4.4 *The E_P equation*

This section gives the formula of the E_P created by the ANN-EFO. Based on Fig. 4, the contribution of the inputs to the output (i.e., the E_P) passes through a complicated

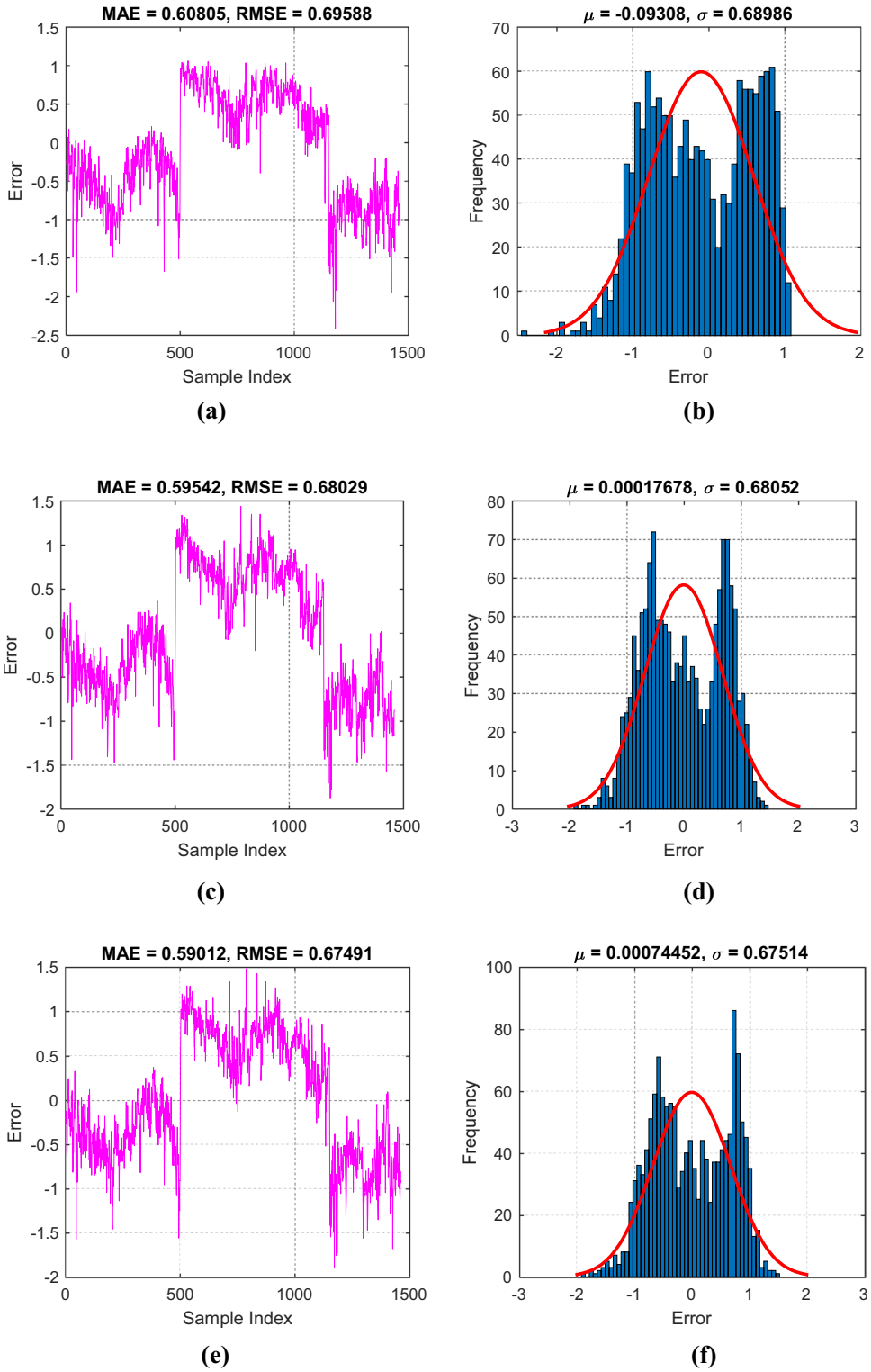

Fig. 6 Training errors for **a**, **b** single ANN, **c**, **d** ANN-SCE, and **e**, **f** ANN-EFO

neural network. It was explained that 36 parameters that are optimized by the EFO are involved in this process. Equation 11 calculates the E_P:

$$E_P = [\mathrm{LW}] \cdot (f(([\mathrm{IW}] \cdot [\mathrm{Input}]) + [b1])) + [b2]. \quad (11)$$

In the above relationship, [LW] is the vector of the hidden-output weights given in Eq. 12, [IW] is the vector of the

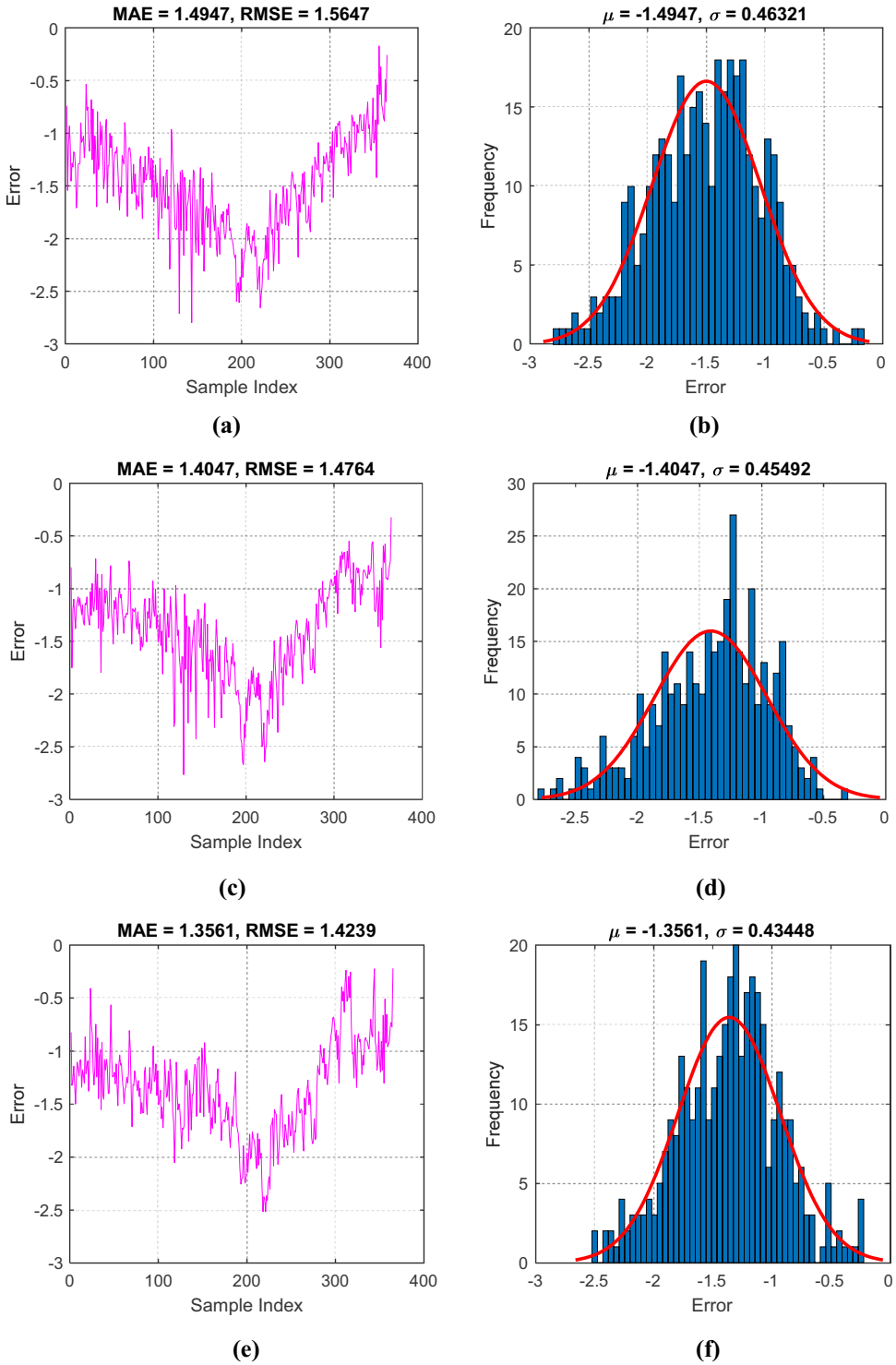

Fig. 7 Testing errors for **a**, **b** single ANN, **c**, **d** ANN-SCE, and **e**, **f** ANN-EFO

input-hidden weights given in Eq. 13, [Input] is the vector of input factors given in Eq. 14, [$b1$] is the vector of hidden biases given in Eq. 15, and [$b2$] is the vector of output bias given in Eq. 16. Also, f denotes the activation function expressed in Eq. 17:

$$\mathrm{LW} = \begin{bmatrix} -0.9935 & 0.3151 & -0.7192 & -0.9814 & -0.1872 \end{bmatrix} \tag{12}$$

$$\mathrm{IW} = \begin{bmatrix} 0.6170 & -0.1241 & 1.1595 & -0.6882 & -1.2317 \\ -1.0706 & -0.2674 & 0.2105 & 0.7013 & -1.4062 \\ 0.1757 & -1.1247 & -0.7690 & 0.9611 & 0.9593 \\ 1.2087 & 0.3759 & 1.0580 & 0.9998 & -0.0992 \\ -1.2847 & -0.6414 & 0.1228 & -1.2334 & -0.3647 \end{bmatrix} \tag{13}$$

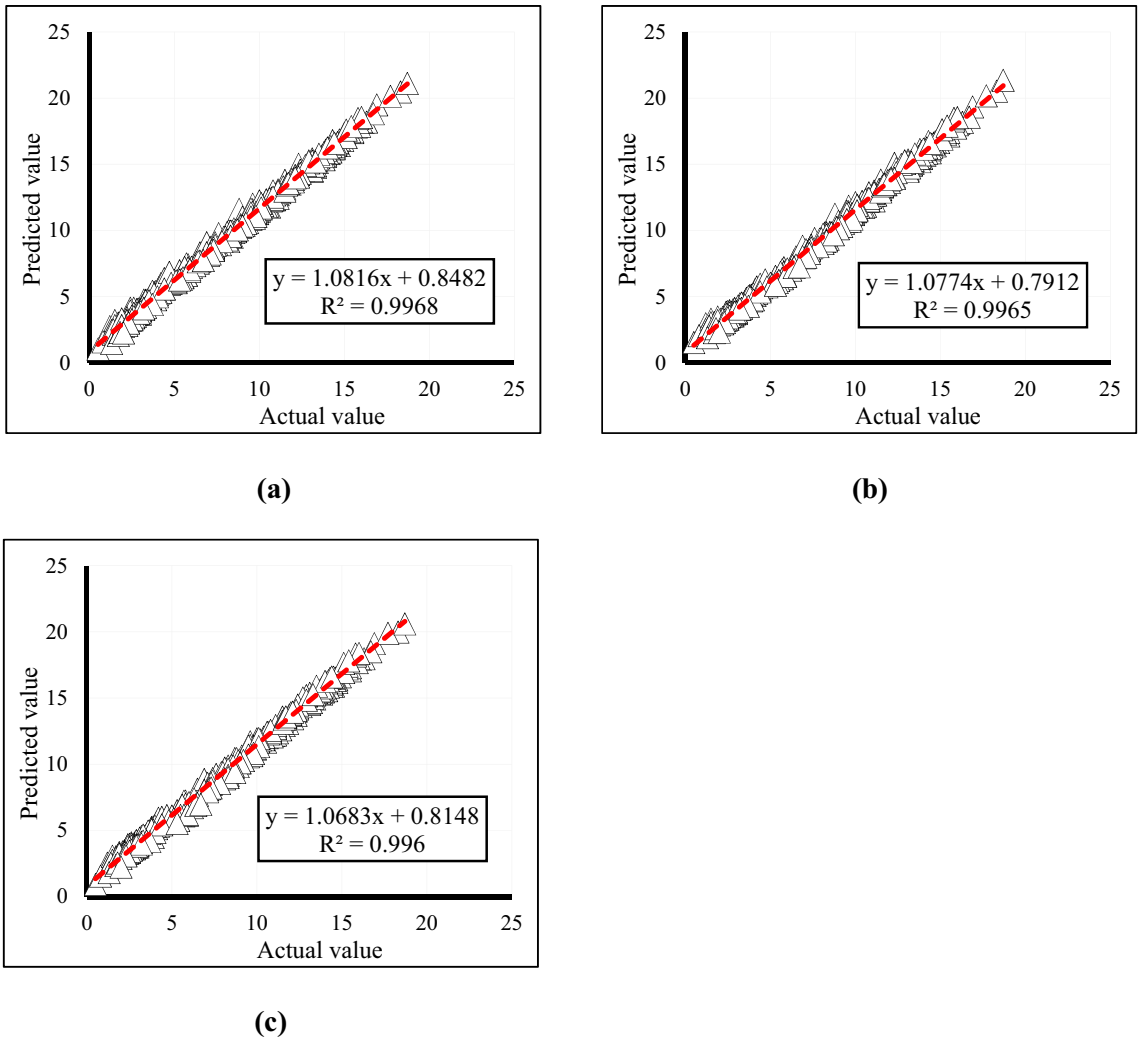

Fig. 8 Regression between the recorded and modeled E_Ps in the testing period after the prediction of **a** single ANN, **b** ANN-SCE, and **c** ANN-EFO

Table 3 Seasonal assessment of the results

Model	R^2			
	Winter	Spring	Summer	Fall
ANN	0.9873	0.9914	0.9937	0.9948
SCE-ANN	0.9906	0.9927	0.9934	0.9930
EFO-ANN	0.9898	0.9962	0.9939	0.9876

$$\text{Input} = \begin{bmatrix} S_W \\ T_A \\ P_D \\ R_S \\ H_D \end{bmatrix} \quad (14)$$

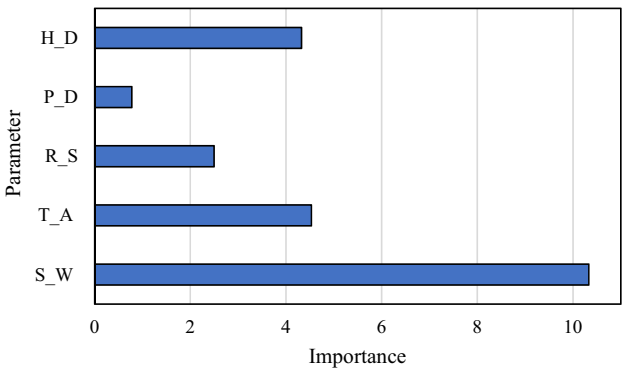

Fig. 9 Importance assessment of the input factors

$$b1 = \begin{bmatrix} -1.9316 \\ 0.9658 \\ 0.0000 \\ 0.9658 \\ -1.9316 \end{bmatrix} \quad (15)$$

$$b2 = \begin{bmatrix} -0.1385 \end{bmatrix} \quad (16)$$

$$f(x) = \frac{2}{1 + e^{-2x}} - 1. \quad (17)$$

According to the above formula, the EFO first creates the appropriate weights and biases to produce some middle parameters in the hidden layer. Next, the outcomes are treated as inputs to produce the final output in the last layer.

4.5 Further discussion

The findings of this paper revealed that the suggested optimizers can be favorably used for pan evaporation modeling through neural network. Apart from accuracy, a significant strength of the used algorithms was their low computation time. It means that both SCE and EFO are able to find an optimal way for the E_P prediction. Back to Fig. 5, while most of metaheuristic optimizers give their best solution with high number of population, the SCE and EFO performed better with small N_Ps. Another appreciable point was the optimization behavior of the EFO which reached a relatively steady situation after 15,000 iteration in the case of this problem. In other words, the EFO has a good potential to improve the established contribution of the input factors for many times. Therefore, the number of iterations should be properly regarded for further applications of this algorithm.

5 Conclusions

The performance of an artificial neural network was supervised by shuffled complex evolution and electromagnetic field optimization toward the optimal prediction of pan evaporation. These algorithms found suitable biases and weights of the ANN in a short time. The quality of their performance was compared to the Levenberg–Marquardt algorithm which is a default trainer for the ANN. It showed that the hybridized ANN can predict the E_P pattern with higher accuracy. For example, the RMSE fell from 1.5647 to 1.4764 after the performance of the SCE. The EFO was even more capable and reduced this value to 1.4239. This advantage, as well the shorter computation time, made the EFO superior over the SCE. It is also a newer strategy. All in all, due to the crucial role of time-efficient accuracy enhancement in engineering simulations, the findings of this study are of interest. Accordingly, testing different metaheuristic strategies on other leading predictive models (e.g., the ANFIS and SVM) in future efforts can improve the E_P modeling in new ways.

Compliance with ethical standards

Conflict of interest The author(s) declare that they have no competing interests.

References

1. Feng W, Lu H, Yao T, Yu Q (2020) Drought characteristics and its elevation dependence in the Qinghai-Tibet plateau during the last half-century. Sci Rep 10:14323. https://doi.org/10.1038/s41598-020-71295-1
2. He L, Shen J, Zhang Y (2018) Ecological vulnerability assessment for ecological conservation and environmental management. J Environ Manag 206:1115–1125. https://doi.org/10.1016/j.jenvman.2017.11.059
3. Hu X, Chong H-Y, Wang X (2019) Sustainability perceptions of off-site manufacturing stakeholders in Australia. J Clean Prod 227:346–354. https://doi.org/10.1016/j.jclepro.2019.03.258
4. Zhang B, Xu D, Liu Y, Li F, Cai J, Du L (2016) Multi-scale evapotranspiration of summer maize and the controlling meteorological factors in north China. Agric For Meteorol 216:1–12. https://doi.org/10.1016/j.agrformet.2015.09.015
5. Seyedashraf O, Mehrabi M, Akhtari AA (2018) Novel approach for dam break flow modeling using computational intelligence. J Hydrol 559:1028–1038
6. Feng S, Lu H, Tian P, Xue Y, Lu J, Tang M, Feng W (2020) Analysis of microplastics in a remote region of the Tibetan Plateau: implications for natural environmental response to human activities. Sci Total Environ 739:140087. https://doi.org/10.1016/j.scitotenv.2020.140087
7. Han X, Zhang D, Yan J, Zhao S, Liu J (2020) Process development of flue gas desulphurization wastewater treatment in coal-fired power plants towards zero liquid discharge: energetic, economic and environmental analyses. J Clean Prod 261:121144. https://doi.org/10.1016/j.jclepro.2020.121144
8. He L, Chen Y, Li J (2018) A three-level framework for balancing the tradeoffs among the energy, water, and air-emission implications within the life-cycle shale gas supply chains. Resour Conserv Recycl 133:206–228. https://doi.org/10.1016/j.resconrec.2018.02.015
9. He L, Chen Y, Zhao H, Tian P, Xue Y, Chen L (2018) Game-based analysis of energy-water nexus for identifying environmental impacts during Shale gas operations under stochastic input. Sci Total Environ 627:1585–1601. https://doi.org/10.1016/j.scitotenv.2018.02.004
10. Wang S, Zhang K, van Beek LPH, Tian X, Bogaard TA (2020) Physically-based landslide prediction over a large region: scaling low-resolution hydrological model results for high-resolution slope stability assessment. Environ Model Softw 124:104607. https://doi.org/10.1016/j.envsoft.2019.104607
11. Yang M, Sowmya A (2015) An underwater color image quality evaluation metric. IEEE Trans Image Process 24:6062–6071. https://doi.org/10.1109/TIP.2015.2491020
12. Zhang K, Ruben GB, Li X, Li Z, Yu Z, Xia J, Dong Z (2020) A comprehensive assessment framework for quantifying climatic

and anthropogenic contributions to streamflow changes: a case study in a typical semi-arid North China basin. Environ Model Softw 128:104704. https://doi.org/10.1016/j.envsoft.2020.104704
13. Lyu Z, Chai J, Xu Z, Qin Y, Cao J (2019) A comprehensive review on reasons for tailings dam failures based on case history. Adv Civ Eng 2019:4159306. https://doi.org/10.1155/2019/4159306
14. Liu J, Liu Y, Wang X (2020) An environmental assessment model of construction and demolition waste based on system dynamics: a case study in Guangzhou. Environ Sci Pollut Res 27:37237–37259. https://doi.org/10.1007/s11356-019-07107-5
15. Chen Y, He L, Guan Y, Lu H, Li J (2017) Life cycle assessment of greenhouse gas emissions and water-energy optimization for shale gas supply chain planning based on multi-level approach: case study in Barnett, Marcellus, Fayetteville, and Haynesville shales. Energy Convers Manag 134:382–398. https://doi.org/10.1016/j.enconman.2016.12.019
16. Li X, Zhang R, Zhang X, Zhu P, Yao T (2020) Silver-catalyzed decarboxylative allylation of difluoroarylacetic acids with allyl sulfones in water. Chem Asian J 15:1175–1179. https://doi.org/10.1002/asia.202000059
17. Chen Y, He L, Li J, Zhang S (2018) Multi-criteria design of shale-gas-water supply chains and production systems towards optimal life cycle economics and greenhouse gas emissions under uncertainty. Comput Chem Eng 109:216–235. https://doi.org/10.1016/j.compchemeng.2017.11.014
18. Yang W, Zhao Y, Wang D, Wu H, Lin A, He L (2020) Using principal components analysis and IDW interpolation to determine spatial and temporal changes of surface water quality of Xin'anjiang river in Huangshan, China. Int J Environ Res Public Health 17:2942
19. Chen Y, Li J, Lu H, Yan P (2021) Coupling system dynamics analysis and risk aversion programming for optimizing the mixed noise-driven shale gas-water supply chains. J Clean Prod 278:123209. https://doi.org/10.1016/j.jclepro.2020.123209
20. Cao B, Zhao J, Lv Z, Gu Y, Yang P, Halgamuge SK (2020) Multiobjective evolution of fuzzy rough neural network via distributed parallelism for stock prediction. IEEE Trans Fuzzy Syst 28:939–952
21. Shi K, Wang J, Tang Y, Zhong S (2020) Reliable asynchronous sampled-data filtering of T-S fuzzy uncertain delayed neural networks with stochastic switched topologies. Fuzzy Sets Syst 381:1–25
22. Shi K, Wang J, Zhong S, Tang Y, Cheng J (2020) Non-fragile memory filtering of T-S fuzzy delayed neural networks based on switched fuzzy sampled-data control. Fuzzy Sets Syst 394:40–64. https://doi.org/10.1016/j.fss.2019.09.001
23. Xu M, Li T, Wang Z, Deng X, Yang R, Guan Z (2018) Reducing complexity of HEVC: a deep learning approach. IEEE Trans Image Process 27:5044–5059. https://doi.org/10.1109/TIP.2018.2847035
24. Yang L, Chen H (2019) Fault diagnosis of gearbox based on RBF-PF and particle swarm optimization wavelet neural network. Neural Comput Appl 31:4463–4478. https://doi.org/10.1007/s00521-018-3525-y
25. Yang S, Deng B, Wang J, Li H, Lu M, Che Y, Wei X, Loparo KA (2020) Scalable digital neuromorphic architecture for large-scale biophysically meaningful neural network with multi-compartment neurons. IEEE Trans Neural Netw Learn Syst 31:148–162. https://doi.org/10.1109/TNNLS.2019.2899936
26. Zhu Q (2020) Research on road traffic situation awareness system based on image big data. IEEE Intell Syst 35:18–26. https://doi.org/10.1109/MIS.2019.2942836
27. Xu L, Jiang S, Zou Q (2020) An in silico approach to identification, categorization and prediction of nucleic acid binding proteins. bioRxiv
28. Nema MK, Khare D, Chandniha SK (2017) Application of artificial intelligence to estimate the reference evapotranspiration in sub-humid Doon valley. Appl Water Sci 7:3903–3910
29. Malik A, Kumar A, Kisi O (2018) Daily pan evaporation estimation using heuristic methods with gamma test. J Irrig Drain Eng 144:04018023
30. Wang L, Niu Z, Kisi O, Yu D (2017) Pan evaporation modeling using four different heuristic approaches. Comput Electron Agric 140:203–213
31. Adnan RM, Malik A, Kumar A, Parmar KS, Kisi O (2019) Pan evaporation modeling by three different neuro-fuzzy intelligent systems using climatic inputs. Arab J Geosci 12:606
32. Abbas MY (2020) Estimating daily evaporation in syrian coast using gene expression programming and adaptive neuro-fuzzy inference system. J Eng Comput Sci (JECS) 21:48–55
33. Kisi O, Heddam S (2019) Evaporation modelling by heuristic regression approaches using only temperature data. Hydrol Sci J 64:653–672
34. Jafari M, Dinpashoh Y (2019) Derivation of regression models for pan evaporation estimation. Environ Resour Res 7:29–42
35. Kisi O, Genc O, Dinc S, Zounemat-Kermani M (2016) Daily pan evaporation modeling using chi-squared automatic interaction detector, neural networks, classification and regression tree. Comput Electron Agric 122:112–117
36. Londhe S, Shah S (2017) Evaluation of pan evaporation model developed using ANN, development of water resources in India. Springer, Berlin, pp 221–231
37. Patle G, Chettri M, Jhajharia D (2020) Monthly pan evaporation modelling using multiple linear regression and artificial neural network techniques. Water Supply 20:800–808
38. Chen J-L, Yang H, Lv M-Q, Xiao Z-L, Wu SJ (2019) Estimation of monthly pan evaporation using support vector machine in Three Gorges Reservoir Area, China. Theor Appl Climatol 138:1095–1107
39. Pammar L, Deka PC (2017) Daily pan evaporation modeling in climatically contrasting zones with hybridization of wavelet transform and support vector machines. Paddy Water Environ 15:711–722
40. Ehteram M, Singh VP, Ferdowsi A, Mousavi SF, Farzin S, Karami H, Mohd NS, Afan HA, Lai SH, Kisi O (2019) An improved model based on the support vector machine and cuckoo algorithm for simulating reference evapotranspiration. PLoS ONE 14:e0217499
41. Cao B, Zhao J, Gu Y, Fan S, Yang P (2020) Security-aware industrial wireless sensor network deployment optimization. IEEE Trans Ind Inform 16:5309–5316. https://doi.org/10.1109/TII.2019.2961340
42. Cao Y, Li Y, Zhang G, Jermsittiparsert K, Nasseri M (2020) An efficient terminal voltage control for PEMFC based on an improved version of whale optimization algorithm. Energy Rep 6:530–542. https://doi.org/10.1016/j.egyr.2020.02.035
43. Gao N, Wu J, Lu K, Zhong H (2021) Hybrid composite metaporous structure for improving and broadening sound absorption. Mechanical Systems and Signal Processing 154: 107504, https://doi.org/10.1016/j.ymssp.2020.107504.
44. Chen H, Qiao H, Xu L, Feng Q, Cai K (2019) A fuzzy optimization strategy for the implementation of RBF LSSVR model in Vis–NIR analysis of pomelo maturity. IEEE Trans Ind Inf 15:5971–5979
45. Liu E, Lv L, Yi Y, Xie P (2019) Research on the steady operation optimization model of natural gas pipeline considering the combined operation of air coolers and compressors. IEEE Access 7:83251–83265. https://doi.org/10.1109/ACCESS.2019.2924515

46. Zhu J, Shi Q, Wu P, Sheng Z, Wang X (2018) Complexity analysis of prefabrication contractors' dynamic price competition in mega projects with different competitive strategies. Complexity 2018, Article ID 5928235, https://doi.org/10.1155/2018/5928235
47. Wu C, Wu P, Wang J, Jiang R, Chen M, Wang X (2020) Critical review of data-driven decision-making in bridge operation and maintenance. Struct Infrastruct Eng. https://doi.org/10.1080/15732479.2020.1833946
48. Zhang C, Abedini M, Mehrmashhadi J (2020) Development of pressure-impulse models and residual capacity assessment of RC columns using high fidelity Arbitrary Lagrangian–Eulerian simulation. Eng Struct 224:111219. https://doi.org/10.1016/j.engstruct.2020.111219
49. Zhang C, Wang H (2020) Swing vibration control of suspended structures using the Active Rotary Inertia Driver system: theoretical modeling and experimental verification. Struct Control Health Monit 27:e2543. https://doi.org/10.1002/stc.2543
50. Alam Z, Zhang C, Samali B (2020) Influence of seismic incident angle on response uncertainty and structural performance of tall asymmetric structure. Structural Design Tall Special Build 29:e1750. https://doi.org/10.1002/tal.1750
51. Li C, Sun L, Xu Z, Wu X, Liang T, Shi W (2020) Experimental Investigation and Error Analysis of High Precision FBG Displacement Sensor for Structural Health Monitoring. Int J Struct Stabi Dyn 20(06):2040011. https://doi.org/10.1142/S0219455420400118
52. Mousavi AA, Zhang C, Masri SF, Gholipour G (2020) Structural Damage Localization and Quantification Based on a CEEMDAN Hilbert Transform Neural Network Approach: A Model Steel Truss Bridge Case Study. Sensors 20:1271. https://doi.org/10.3390/s20051271
53. Alam Z, Zhang C, Samali B (2020) The role of viscoelastic damping on retrofitting seismic performance of asymmetric reinforced concrete structures. Earthquake Eng Eng Vib 19:223–237. https://doi.org/10.1007/s11803-020-0558-x
54. Wang J, Zhu P, He B, Deng G, Zhang C, Huang X (2020) An Adaptive Neural Sliding Mode Control with ESO for Uncertain Nonlinear Systems. Int J Control Autom Syst. https://doi.org/10.1007/s12555-019-0972-x
55. Zhang C, Alam Z, Sun L, Su Z, Samali B (2019) Fibre Bragg grating sensor-based damage response monitoring of an asymmetric reinforced concrete shear wall structure subjected to progressive seismic loads. Struct Control Health Monit 26:e2307. https://doi.org/10.1002/stc.2307
56. Zhang C, Gholipour G, Mousavi AA (2020) Blast loads induced responses of RC structural members: State-of-the-art review. Compos Part B: Eng 195:108066. https://doi.org/10.1016/j.compositesb.2020.108066
57. Chao M, Kai C, Zhiwei Z (2020) Research on tobacco foreign body detection device based on machine vision. Trans Inst Meas Control 42:2857–2871. https://doi.org/10.1177/0142331220929816
58. Zhang H, Qu S, Li H, Luo J, Xu W (2020) A moving shadow elimination method based on fusion of multi-feature. IEEE Access 8:63971–63982. https://doi.org/10.1109/ACCESS.2020.2984680
59. Mi C, Cao L, Zhang Z, Feng Y, Yao L, Wu Y (2020) A port container code recognition algorithm under natural conditions. J Coast Res 103:822–829. https://doi.org/10.2112/SI103-170.1
60. Yue H, Wang H, Chen H, Cai K, Jin Y (2020) Automatic detection of feather defects using Lie group and fuzzy Fisher criterion for shuttlecock production. Mech Syst Signal Process 141:106690. https://doi.org/10.1016/j.ymssp.2020.106690
61. Zenggang X, Zhiwen T, Xiaowen C, Xue-min Z, Kaibin Z, Conghuan Y (2019) Research on image retrieval algorithm based on combination of color and shape features. J Signal Process Syst. https://doi.org/10.1007/s11265-019-01508-y
62. Wang Y, Yuan Y, Wang Q, Liu C, Zhi Q, Cao J (2020) Changes in air quality related to the control of coronavirus in China: implications for traffic and industrial emissions. Sci Total Environ 731:139133. https://doi.org/10.1016/j.scitotenv.2020.139133
63. Zhang Y, Huang P (2019) Influence of mine shallow roadway on airflow temperature. Arab J Geosci 13:12. https://doi.org/10.1007/s12517-019-4934-7
64. Deng Y, Zhang T, Clark J, Aminabhavi T, Kruse A, Tsang DC, Sharma BK, Zhang F, Ren H (2020) Mechanisms and modelling of phosphorus solid–liquid transformation during the hydrothermal processing of swine manure. Green Chem 22:5628–5638. https://doi.org/10.1039/D0GC01281E
65. Zhou G, Moayedi H, Foong LK (2020) Teaching–learning-based metaheuristic scheme for modifying neural computing in appraising energy performance of building. Engineering with Computers 35:1–12. https://doi.org/10.1007/s00366-020-00981-5
66. Zhang W (2020) Parameter adjustment strategy and experimental development of hydraulic system for wave energy power generation. Symmetry 12:711
67. Fu X, Fortino G, Pace P, Aloi G, Li W (2020) Environment-fusion multipath routing protocol for wireless sensor networks. Inf Fusion 53:4–19. https://doi.org/10.1016/j.inffus.2019.06.001
68. Yan J, Pu W, Zhou S, Liu H, Bao Z (2020) Collaborative detection and power allocation framework for target tracking in multiple radar system. Inf Fusion 55:173–183. https://doi.org/10.1016/j.inffus.2019.08.010
69. Liu E, Guo B, Lv L, Qiao W, Azimi M (2020) Numerical simulation and simplified calculation method for heat exchange performance of dry air cooler in natural gas pipeline compressor station. Energy Sci Eng 8:2256–2270. https://doi.org/10.1002/ese3.661
70. Liu E, Wang X, Zhao W, Su Z, Chen Q (2020) Analysis and Research on Pipeline Vibration of a Natural Gas Compressor Station and Vibration Reduction Measures. Energy Fuels. https://doi.org/10.1021/acs.energyfuels.0c03663
71. Peng S, Chen Q, Zheng C, Liu E (2020) Analysis of particle deposition in a new-type rectifying plate system during shale gas extraction. Energy Sci Eng 8:702–717. https://doi.org/10.1002/ese3.543
72. Wang S-J, Chen H-L, Yan W-J, Chen Y-H, Fu X (2014) Face recognition and micro-expression recognition based on discriminant tensor subspace analysis plus extreme learning machine. Neural Process Lett 39:25–43. https://doi.org/10.1007/s11063-013-9288-7
73. Zhang X, Fan M, Wang D, Zhou P, Tao D (2020) Top-k feature selection framework using robust 0–1 integer programming. IEEE Trans Neural Netw Learn Syst. https://doi.org/10.1109/TNNLS.2020.3009209
74. Zhang X, Jiang R, Wang T, Wang J (2020) Recursive neural network for video deblurring. IEEE Trans Circ Syst Video Technol. https://doi.org/10.1109/TCSVT.2020.3035722
75. Zhang X, Wang T, Wang J, Tang G, Zhao L (2020) Pyramid channel-based feature attention network for image dehazing. Comput Vis Image Underst. https://doi.org/10.1016/j.cviu.2020.103003
76. Xu S, Wang J, Shou W, Ngo T, Sadick A-M, Wang X (2020) Computer vision techniques in construction: a critical review. Arch Comput Methods Eng. https://doi.org/10.1007/s11831-020-09504-3
77. Zuo C, Chen Q, Tian L, Waller L, Asundi A (2015) Transport of intensity phase retrieval and computational imaging for partially coherent fields: the phase space perspective. Opt Lasers Eng 71:20–32. https://doi.org/10.1016/j.optlaseng.2015.03.006

78. Xu M, Li C, Zhang S, Callet PL (2020) State-of-the-art in 360° video/image processing: perception, assessment and compression. IEEE J Sel Top Signal Process 14:5–26. https://doi.org/10.1109/JSTSP.2020.2966864
79. He L, Shao F, Ren L (2020) Sustainability appraisal of desired contaminated groundwater remediation strategies: an information-entropy-based stochastic multi-criteria preference model. Environ Dev Sustain. https://doi.org/10.1007/s10668-020-00650-z
80. Liu Y, Yang C, Sun Q (2020) Thresholds based image extraction schemes in big data environment in intelligent traffic management. IEEE Trans Intell Transp Syst. https://doi.org/10.1109/TITS.2020.2994386
81. Sun Y, Wang J, Wu J, Shi W, Ji D, Wang X, Zhao X (2020) Constraints hindering the development of high-rise modular buildings. Appl Sci 10:7159. https://doi.org/10.3390/app10207159
82. Zhu L, Kong L, Zhang C (2020) Numerical study on hysteretic behaviour of horizontal-connection and energy-dissipation structures developed for prefabricated shear walls. Appl Sci 10:1240. https://doi.org/10.3390/app10041240
83. Abedini M, Zhang C (2020) Performance assessment of concrete and steel material models in LS-DYNA for enhanced numerical simulation, a state of the art review. Arch Comput Methods Eng. https://doi.org/10.1007/s11831-020-09483-
84. Xiong Z, Xiao N, Xu F, Zhang X, Xu Q, Zhang K, Ye C (2020) An equivalent exchange based data forwarding incentive scheme for socially aware networks. J Signal Process Syst. https://doi.org/10.1007/s11265-020-01610-6
85. Tian P, Lu H, Feng W, Guan Y, Xue Y (2020) Large decrease in streamflow and sediment load of Qinghai-Tibetan Plateau driven by future climate change: a case study in Lhasa River Basin. CATENA 187:104340. https://doi.org/10.1016/j.catena.2019.104340
86. Lu H, Tian P, He L (2019) Evaluating the global potential of aquifer thermal energy storage and determining the potential worldwide hotspots driven by socio-economic, geo-hydrologic and climatic conditions. Renew Sustain Energy Rev 112:788–796. https://doi.org/10.1016/j.rser.2019.06.013
87. Shi K, Wang J, Zhong S, Tang Y, Cheng J (2020) Non-fragile memory filtering of TS fuzzy delayed neural networks based on switched fuzzy sampled-data control. Fuzzy Sets Syst 394:40–64
88. Chen H, Heidari AA, Chen H, Wang M, Pan Z, Gandomi AH (2020) Multi-population differential evolution-assisted Harris hawks optimization: framework and case studies. Future Gener Comput Syst 111:175–198. https://doi.org/10.1016/j.future.2020.04.008
89. Hu L, Hong G, Ma J, Wang X, Chen H (2015) An efficient machine learning approach for diagnosis of paraquat-poisoned patients. Comput Biol Med 59:116–124. https://doi.org/10.1016/j.compbiomed.2015.02.003
90. Liu D, Wang S, Huang D, Deng G, Zeng F, Chen H (2016) Medical image classification using spatial adjacent histogram based on adaptive local binary patterns. Comput Biol Med 72:185–200. https://doi.org/10.1016/j.compbiomed.2016.03.010
91. Wang M, Chen H (2020) Chaotic multi-swarm whale optimizer boosted support vector machine for medical diagnosis. Appl Soft Comput J. https://doi.org/10.1016/j.asoc.2019.105946
92. Xia J, Chen H, Li Q, Zhou M, Chen L, Cai Z, Fang Y, Zhou H (2017) Ultrasound-based differentiation of malignant and benign thyroid nodules: an extreme learning machine approach. Comput Methods Programs Biomed 147:37–49. https://doi.org/10.1016/j.cmpb.2017.06.005
93. Xu Y, Chen H, Luo J, Zhang Q, Jiao S, Zhang X (2019) Enhanced Moth-flame optimizer with mutation strategy for global optimization. Inf Sci 492:181–203. https://doi.org/10.1016/j.ins.2019.04.022
94. Zhao X, Zhang X, Cai Z, Tian X, Wang X, Huang Y, Chen H, Hu L (2019) Chaos enhanced grey wolf optimization wrapped ELM for diagnosis of paraquat-poisoned patients. Comput Biol Chem 78:481–490. https://doi.org/10.1016/j.compbiolchem.2018.11.017
95. Li C, Hou L, Sharma BY, Li H, Chen C, Li Y, Zhao X, Huang H, Cai Z, Chen H (2018) Developing a new intelligent system for the diagnosis of tuberculous pleural effusion. Comput Methods Programs Biomed 153:211–225. https://doi.org/10.1016/j.cmpb.2017.10.022
96. Fu X, Pace P, Aloi G, Yang L, Fortino G (2020) Topology optimization against cascading failures on wireless sensor networks using a memetic algorithm. Comput Netw 107327
97. Wu T, Cao J, Xiong L, Zhang H (2019) New stabilization results for semi-Markov chaotic systems with fuzzy sampled-data control. Complexity 2019:7875305. https://doi.org/10.1155/2019/7875305
98. Chen H-L, Wang G, Ma C, Cai Z-N, Liu W-B, Wang S-J (2016) An efficient hybrid kernel extreme learning machine approach for early diagnosis of Parkinson's disease. Neurocomputing 184:131–144. https://doi.org/10.1016/j.neucom.2015.07.138
99. Shen L, Chen H, Yu Z, Kang W, Zhang B, Li H, Yang B, Liu D (2016) Evolving support vector machines using fruit fly optimization for medical data classification. Knowl Based Syst 96:61–75. https://doi.org/10.1016/j.knosys.2016.01.002
100. Xu X, Chen H-L (2014) Adaptive computational chemotaxis based on field in bacterial foraging optimization. Soft Comput 18:797–807. https://doi.org/10.1007/s00500-013-1089-4
101. Cao B, Dong W, Lv Z, Gu Y, Singh S, Kumar P (2020) Hybrid microgrid many-objective sizing optimization with fuzzy decision. IEEE Trans Fuzzy Syst 28:2702–2710
102. Cao B, Wang X, Zhang W, Song H, Lv Z (2020) A many-objective optimization model of industrial internet of things based on private blockchain. IEEE Netw 34:78–83
103. Cao B, Fan S, Zhao J, Yang P, Muhammad K, Tanveer M (2020) Quantum-enhanced multiobjective large-scale optimization via parallelism. Swarm Evol Comput 57:100697. https://doi.org/10.1016/j.swevo.2020.100697
104. Cao B, Zhao J, Gu Y, Ling Y, Ma X (2020) Applying graph-based differential grouping for multiobjective large-scale optimization. Swarm Evol Comput 53:100626. https://doi.org/10.1016/j.swevo.2019.100626
105. Zhang Y, Liu R, Wang X, Chen H, Li C (2020) Boosted binary Harris hawks optimizer and feature selection. Eng Comput. https://doi.org/10.1007/s00366-020-01028-5
106. Qu S, Han Y, Wu Z, Raza H (2020) Consensus modeling with asymmetric cost based on data-driven robust optimization. Group Decis Negot. https://doi.org/10.1007/s10726-020-09707-w
107. Cao B, Zhao J, Yang P, Gu Y, Muhammad K, Rodrigues JJPC, Albuquerque VHCd (2020) Multiobjective 3-D topology optimization of next-generation wireless data center network. IEEE Trans Ind Inf 16:3597–3605. https://doi.org/10.1109/TII.2019.2952565
108. Sun G, Yang B, Yang Z, Xu G (2019) An adaptive differential evolution with combined strategy for global numerical optimization. Soft Comput. https://doi.org/10.1007/s00500-019-03934-3
109. Wang M, Chen H, Yang B, Zhao X, Hu L, Cai Z, Huang H, Tong C (2017) Toward an optimal kernel extreme learning machine using a chaotic moth-flame optimization strategy with applications in medical diagnoses. Neurocomputing 267:69–84. https://doi.org/10.1016/j.neucom.2017.04.060
110. Chen H, Chen A, Xu L, Xie H, Qiao H, Lin Q, Cai K (2020) A deep learning CNN architecture applied in smart near-infrared analysis of water pollution for agricultural irrigation resources. Agric Water Manag 240:106303

111. Qian J, Feng S, Li Y, Tao T, Han J, Chen Q, Zuo C (2020) Single-shot absolute 3D shape measurement with deep-learning-based color fringe projection profilometry. Opt Lett 45:1842–1845
112. Lv Z, Qiao L (2020) Deep belief network and linear perceptron based cognitive computing for collaborative robots. Appl Soft Comput 92:106300. https://doi.org/10.1016/j.asoc.2020.106300
113. Qian J, Feng S, Tao T, Hu Y, Li Y, Chen Q, Zuo C (2020) Deep-learning-enabled geometric constraints and phase unwrapping for single-shot absolute 3D shape measurement. APL Photon 5:046105. https://doi.org/10.1063/5.0003217
114. Li T, Xu M, Zhu C, Yang R, Wang Z, Guan Z (2019) A deep learning approach for multi-frame in-loop filter of HEVC. IEEE Trans Image Process 28:5663–5678. https://doi.org/10.1109/TIP.2019.2921877
115. Zhao X, Li D, Yang B, Chen H, Yang X, Yu C, Liu S (2015) A two-stage feature selection method with its application. Comput Electr Eng 47:114–125. https://doi.org/10.1016/j.compeleceng.2015.08.011
116. Zhao X, Li D, Yang B, Ma C, Zhu Y, Chen H (2014) Feature selection based on improved ant colony optimization for online detection of foreign fiber in cotton. Appl Soft Comput 24:585–596. https://doi.org/10.1016/j.asoc.2014.07.024
117. Xiong Q, Zhang X, Wang W-F, Gu Y (2020) A parallel algorithm framework for feature extraction of EEG signals on MPI. Comput Math Methods Med 2020:9812019. https://doi.org/10.1155/2020/9812019
118. Zhang J, Liu B (2019) A review on the recent developments of sequence-based protein feature extraction methods. Curr Bioinform 14:190–199
119. Qiu T, Shi X, Wang J, Li Y, Qu S, Cheng Q, Cui T, Sui S (2019) Deep learning: a rapid and efficient route to automatic metasurface design. Adv Sci 6:1900128. https://doi.org/10.1002/advs.201900128
120. Arunkumar R, Jothiprakash V, Sharma K (2017) Artificial intelligence techniques for predicting and mapping daily pan evaporation. J Inst Eng (India) Ser A 98:219–231
121. Alsumaiei AA (2020) Utility of artificial neural networks in modeling pan evaporation in hyper-arid climates. Water 12:1508
122. Ghaemi A, Rezaie-Balf M, Adamowski J, Kisi O, Quilty J (2019) On the applicability of maximum overlap discrete wavelet transform integrated with MARS and M5 model tree for monthly pan evaporation prediction. Agric For Meteorol 278:107647
123. Keshtegar B, Heddam S, Sebbar A, Zhu S-P, Trung N-T (2019) SVR-RSM: a hybrid heuristic method for modeling monthly pan evaporation. Environ Sci Pollut Res 26:35807–35826
124. Moayedi H, Mehrabi M, Kalantar B, AbdullahiMuazu M, Rashid AAS, Foong LK, Nguyen H (2019) Novel hybrids of adaptive neuro-fuzzy inference system (ANFIS) with several metaheuristic algorithms for spatial susceptibility assessment of seismic-induced landslide. Geom Nat Hazards Risk 10:1879–1911
125. Roy DK, Barzegar R, Quilty J, Adamowski J (2020) Using ensembles of adaptive neuro-fuzzy inference system and optimization algorithms to predict reference evapotranspiration in subtropical climatic zones. J Hydrol 591:125509. https://doi.org/10.1016/j.jhydrol.2020.125509
126. Gocić M, Motamedi S, Shamshirband S, Petković D, Ch S, Hashim R, Arif M (2015) Soft computing approaches for forecasting reference evapotranspiration. Comput Electron Agric 113:164–173
127. Mohammadi B, Mehdizadeh S (2020) Modeling daily reference evapotranspiration via a novel approach based on support vector regression coupled with whale optimization algorithm. Agric Water Manag 237:106145. https://doi.org/10.1016/j.agwat.2020.106145
128. Liu J, Wu C, Wu G, Wang X (2015) A novel differential search algorithm and applications for structure design. Appl Math Comput 268:246–269
129. Petković D, Gocic M, Shamshirband S, Qasem SN, Trajkovic S (2016) Particle swarm optimization-based radial basis function network for estimation of reference evapotranspiration. Theor Appl Climatol 125:555–563
130. Cheng X, He L, Lu H, Chen Y, Ren L (2016) Optimal water resources management and system benefit for the Marcellus shale-gas reservoir in Pennsylvania and West Virginia. J Hydrol 540:412–422. https://doi.org/10.1016/j.jhydrol.2016.06.041
131. Peng S, Zhang Z, Liu E, Liu W, Qiao W (2021) A new hybrid algorithm model for prediction of internal corrosion rate of multiphase pipeline. J Nat Gas Sci Eng 85:103716. https://doi.org/10.1016/j.jngse.2020.103716
132. Ashrafzadeh A, Malik A, Jothiprakash V, Ghorbani MA, Biazar SM (2018) Estimation of daily pan evaporation using neural networks and meta-heuristic approaches. ISH J Hydraul Eng 26(4):421–429. https://doi.org/10.1080/09715010.2018.1498754
133. Tikhamarine Y, Malik A, Kumar A, Souag-Gamane D, Kisi O (2019) Estimation of monthly reference evapotranspiration using novel hybrid machine learning approaches. Hydrol Sci J 64:1824–1842
134. Seifi A, Soroush F (2020) Pan evaporation estimation and derivation of explicit optimized equations by novel hybrid meta-heuristic ANN based methods in different climates of Iran. Comput Electron Agric 173:105418
135. Bouchekara H (2020) Solution of the optimal power flow problem considering security constraints using an improved chaotic electromagnetic field optimization algorithm. Neural Comput Appl 32:2683–2703
136. Zhang C-W, Ou J-P, Zhang J-Q (2006) Parameter optimization and analysis of a vehicle suspension system controlled by magnetorheological fluid dampers. Struct Control Health Monit 13:885–896. https://doi.org/10.1002/stc.63
137. Cobaner M (2013) Reference evapotranspiration based on Class A pan evaporation via wavelet regression technique. Irrig Sci 31:119–134
138. Duan Q, Gupta VK, Sorooshian S (1993) Shuffled complex evolution approach for effective and efficient global minimization. J Optim Theory Appl 76:501–521
139. Duan Q, Sorooshian S, Gupta VK (1994) Optimal use of the SCE-UA global optimization method for calibrating watershed models. J Hydrol 158:265–284
140. Moosavian N, Jaefarzadeh MR (2014) Hydraulic analysis of water distribution network using shuffled complex evolution. J Fluids. https://doi.org/10.1155/2014/979706
141. Ira J, Hasalová L, Jahoda M (2015) The use of optimization in fire development modeling, the use of optimization techniques for estimation of pyrolysis model input parameters. Application of Structural Fire Engineering, 19-20 April 2013, Prague, Czech Republic
142. Gao X, Cui Y, Hu J, Xu G, Wang Z, Qu J, Wang H (2018) Parameter extraction of solar cell models using improved shuffled complex evolution algorithm. Energy Convers Manag 157:460–479. https://doi.org/10.1016/j.enconman.2017.12.033
143. Abedinpourshotorban H, Shamsuddin SM, Beheshti Z, Jawawi DN (2016) Electromagnetic field optimization: a physics-inspired metaheuristic optimization algorithm. Swarm Evol Comput 26:8–22
144. Bouchekara H, Zellagui M, Abido MA (2017) Optimal coordination of directional overcurrent relays using a modified electromagnetic field optimization algorithm. Appl Soft Comput 54:267–283. https://doi.org/10.1016/j.asoc.2017.01.037
145. AbouOmar MS, Su Y-X, Zhang H-J (2019) Hybrid feedback-feedforward fuzzy control of PEM fuel cell air feed system with electromagnetic field optimization. IETE J Res 1–17

146. Song S, Jia H, Ma J (2019) A chaotic electromagnetic field optimization algorithm based on fuzzy entropy for multilevel thresholding color image segmentation. Entropy 21:398
147. Nguyen H, Mehrabi M, Kalantar B, Moayedi H, Mu'azu MA, (2019) Potential of hybrid evolutionary approaches for assessment of geo-hazard landslide susceptibility mapping. Geom Nat Hazards Risk 10:1667–1693
148. Wu C, Wu P, Wang J, Jiang R, Chen M, Wang X (2021) Ontological knowledge base for concrete bridge rehabilitation project management. Automation in Construction 121:103428. https://doi.org/10.1016/j.autcon.2020.103428
149. Yang S, Deng B, Wang J, Li H, Lu M, Che Y, Wei X, Loparo KA (2019) Scalable digital neuromorphic architecture for large-scale biophysically meaningful neural network with multi-compartment neurons. IEEE Trans Neural Netw Learn Syst 31:148–162
150. Zhang H, Qiu Z, Cao J, Abdel-Aty M, Xiong L (2019) Event-triggered synchronization for neutral-type semi-Markovian neural networks with partial mode-dependent time-varying delays. IEEE Trans Neural Netw Learn Syst
151. Moré JJ (1978) The Levenberg–Marquardt algorithm: implementation and theory, numerical analysis. Springer, Berlin, pp 105–116
152. Velasco AC, Darbas M, Mendoza R, Bacon M, de Leon JC (2020) Comparative study of heuristic algorithms for electrical impedance tomography. Philipp J Sci 149:747–761
153. Ye X, Moayedi H, Khari M, Foong LK (2020) Metaheuristic-hybridized multilayer perceptron in slope stability analysis. Smart Struct Syst 26:263–275
154. Moayedi H, Bui DT, Thi Ngo PT (2020) Shuffled frog leaping algorithm and wind-driven optimization technique modified with multilayer perceptron. Appl Sci 10:689
155. Zheng S, Lyu Z, Foong LK (2020) Early prediction of cooling load in energy-efficient buildings through novel optimizer of shuffled complex evolution. Eng Comput 34:1–15. https://doi.org/10.1007/s00366-020-01140-6